POSTMORTEM FRACTURE SURFACE TOPOGRAPHY: AN INVESTIGATION INTO DIFFERENTIATING PERIMORTEM AND POSTMORTEM LONG BONE BLUNT FORCE TRAUMA FRACTURES

by

Kelsee C. Hentschel, B.S.

A thesis submitted to the Graduate Council of
Texas State University in partial fulfillment
of the requirements for the degree of
Master of Arts
with a Major in Anthropology
August 2014

Committee Members:

Daniel J. Wescott, Chair

Michelle D. Hamilton

M. Katherine Spradley

Alberto Giordano

FAIR USE AND AUTHOR'S PERMISSION STATEMENT

Fair Use

Duplication Permission

ACKNOWLEDGEMENTS

First and foremost, I would like to thank the members of my committee for providing me with their encouragement, help, advice, and knowledge throughout this thesis experience. I would like to express my sincerest thanks to my thesis advisor, Dr. Danny Wescott, for all of his help and support throughout this thesis debacle. As I've told you many times, you are awesome. I would also like to thank Dr. Alberto Giordano for all of his help navigating the vast world of Geographic Information Systems, and for being patient with me while I learned his craft. Many thanks also go to Dr. Kate Spradley and Dr. Michelle Hamilton for their time and helpful critiques!

I could not have survived graduate school without my friends and cohort members. Your support and encouragement, if only over a Thursday night beer, kept me sane throughout my graduate career, and I thank you all.

Finally, my greatest thanks goes out to my parents, Cathy and Brian, my sisters, Amanda and Caitlyn, and my grandmother, Mary, for all of their unwavering support and love throughout this entire process. You all have encouraged me and believed in me, and I cannot emphasize enough my appreciation for your patience with me throughout the past two years.

TABLE OF CONTENTS

Page

LIST OF TABLES

Table **Page**

LIST OF FIGURES

Figure **Page**

CHAPTER I

Introduction

Forensic anthropologists are frequently asked to estimate the timing of bone fractures in medicolegal cases to aid in determining the cause and manner of death (Sauer, 1998; Dirmaat et al., 2008). Using fracture characteristics of bone, forensic anthropologists typically report the timing of bone fractures as occurring antemortem (before death), perimortem (around the time of death), or postmortem (after death) (Ubelaker and Adams, 1995; Wheatley, 2008; Wieberg and Wescott, 2008). Since perimortem fractures occur around the time of death, they are usually associated with the death event. Therefore, identification of perimortem fractures is important because it may shed light on the circumstances surrounding an individual's death.

Antemortem fractures can usually be determined if there is evidence of healing. Perimortem and postmortem fractures, however, will not exhibit signs of healing (Ubelaker and Adams, 1995; Sauer, 1998), and therefore, distinguishing between perimortem and postmortem fractures is a much more difficult task for forensic anthropologists. While certain gross characteristics of the fracture can provide clues to distinguish perimortem from postmortem blunt force fractures, it is still difficult to determine the timing of fractures (Shattuck, 2010; Wieberg and Wescott, 2008).

Many authors have noted that the distinction between perimortem and postmortem fractures is largely shaped by the qualities of the bone tissue rather than the timing of the injury (Ubelaker and Adams, 1995; Galloway et al., 1999; Wieberg and Wescott, 2008). Assessment of perimortem and postmortem fractures are often based on

whether the bone was “green” (fresh) or dry at the time of fracture (Johnson, 1985; Ubelaker and Adams, 1995). However, since the decomposition and drying of bone is a continuous process, assigning a fracture to a discrete category (i.e. wet or dry fracture) becomes problematic. As a result, there is a need to develop a method that allows forensic anthropologists to reliably differentiate between perimortem and postmortem fractures.

The aim of my research is to establish if fracture surface morphology can be consistently used to differentiate between wet (perimortem) and dry (postmortem) bone fractures by examining the tension fracture surface. The questions addressed by my research are: 1) is there a quantifiable difference in the tension fracture surface of bones broken at the time of death (postmortem interval (PMI)=0 days) and those broken after death, 2) are there any visible changes in tension fracture surface characteristics as bones progress through the postmortem interval, and 3) can the timing of fractures be recognized based on fracture surface characteristics.

The purpose of this study is to develop a novel method based on tension fracture surface topography that can be used by forensic anthropologists to distinguish between perimortem and postmortem long bone fractures in medicolegal death investigations. Since perimortem fractures are usually associated with the death event or manner of death, the identification of fracture timing is important because it may shed light on the circumstances surrounding an individual’s death. I hope to develop criteria specific to fracture surface morphology that may be used to help establish the timing of the fracturing incident.

In this study I examined the tension fracture surface topography of pig bones broken near the time of death and at different, known periods throughout the postmortem interval. First, I produced 3D images of the fracture surfaces using a NextEngine© 3D laser scanner and used Geographic Information Systems (GIS) to model the fracture surfaces as topographical landscapes. I then analyzed the spatial relationships of the features on the fracture surfaces to determine if there is a relationship between the timing of the fracture and the fracture surface topography. Any significant trends in surface topography will be used to develop model fracture surfaces that can be used by forensic anthropologists to distinguish the timing of long bone fractures.

My research is important because it will potentially provide a new, cost-effective method for forensic anthropologists to distinguish between fresh (perimortem) and dry (postmortem) bone fractures in medicolegal death investigations. A NextEngine© 3D scanner is available for about $3,000 (NextEngine, 2011), and can be invaluable to an anthropology lab. Its scanning ability is not limited to small fracture surfaces; in fact, it can be used to scan entire bones, projectile points, and other artifacts for study (NextEngine, 2011). In addition, GIS software programs are often available for free if the user is a student or professor in a university setting. Therefore, this method for distinguishing the timing of injuries may prove to be a very valuable, cost-effective resource for forensic anthropologists.

The importance of standardized methodologies in the forensic sciences is emphasized by the 1993 *Daubert* ruling, which established guidelines for the admissibility of expert testimony in court. In particular, the *Daubert* ruling (1993) underscored the need for research to have empirically grounded methods, known error

rates, peer review, and acceptance within the scientific community. The current research project will aid forensic anthropologists who may have to testify in court by creating a way to calibrate or measure a fracture characteristic used to identify fracture timing.

In addition, determining the timing of fractures can be useful not only to forensic anthropologists, but also to paleoanthropologists, bioarchaeologists, and paleopathologists. For instance, understanding fracture timing may help distinguish between hominid-modified bones and bones modified by other natural agencies. To elaborate, this research may help determine if faunal bone assemblages from archaeological sites were actively butchered and/or modified by hominids, or if bones were broken from weathering, trampling, or other natural causes. Therefore, this research has the potential to be applicable to many fields of scientific study rather than just forensic anthropology.

The following section provides an overview of the theoretical framework used in trauma analysis. In this section I will discuss the relationship between loading and deformation as well as bone structure and fracture production. I will also discuss the methods used to determine the timing of fractures. This information is necessary to understand the research design and methods used in this study.

Literature Review

Bone Biology and Fracture Production

Bone is a composite material made up of both organic (mostly collagen) and mineral (hydroxyapatite) components that together give it its versatile properties. Bone is viscoelastic and anisotropic, meaning that it is both elastic and stiff and it will respond

differently depending on the forces acting upon it (Johnson, 1985; Kroman and Symes, 2013). The hydroxyapatite gives bone its hardness and rigidity, while collagen is a connective tissue that gives bone its elasticity and flexibility. This mixture of properties allows bones to be rigid enough to support the body while having enough flexibility to resist forces placed upon it (Galloway, 1999; Hiller et al., 2003; Smith et al., 2003; White et al., 2012).

Blunt force trauma refers to injuries sustained from a force that has a large area of contact with the bone, and usually occurs at a low velocity (Galloway, 1999). This type of skeletal trauma usually results from fists, sticks, clubs, motor vehicle accidents, pedestrian accidents, and falls (Galloway, 1999; Smith et al., 2003). Blunt force trauma has a wide range of fracture patterns that depend on several intrinsic and extrinsic factors (Galloway, 1999; Moraitis and Spiliopoulou, 2006). Intrinsic factors are those material and structural properties of bone that influence fracturing (Gonza, 1982). Bone morphology, structural integrity, stiffness and density, and the capacity of the bone to absorb and dissipate energy are intrinsic factors. For instance, cortical bone consists of secondary osteons and collagen fibers that are oriented along the long axis of the bone; this orientation dictates how bone reacts when stressed (Johnson, 1985). In addition, Currey (1959) and Evans (1957) found that the tensile strength of bone decreases as the number of osteons increases. Extrinsic factors such as the shape, mass, and velocity of the instrument applying the force, as well as the direction, rate of loading, and the duration of the forces applied also affects how the bone fractures (Galloway, 1999; Smith et al., 2003).

Fracture production is explained in terms of the load and deformation. Load is the application of force (mass x acceleration) to an object, while deformation is the dimensional change in the object as a result of the load. A force applied to bone causes it to pass through several stages of change: elastic deformation, plastic deformation, and fracture. During elastic deformation the deformation is proportional to the forces applied. In this stage, the bone will return to its natural shape once the load is removed. However, if the load increases, the bone will hit its yield point and enter into plastic deformation. In plastic deformation, bonds between the atoms of the material are irreversibly deformed and broken, and the bone can no longer return to its original shape once the load is removed. Once the deformation caused by the load becomes too great, the bone can no longer accommodate the dimensional change and failure (fracture) will occur. Failure begins with microcracking along the cement lines that surround osteons, and fracture lines tend to follow the cement lines (Evans, 1973; Johnson, 1985).

Types of Forces and Associated Fracture Patterns

The primary forces involved in fracturing are tension, compression, shearing, rotation, and angulation (Figure 1.1). Tension is the "pulling apart" of bone, whereas compression is the compaction of bone (Galloway, 1999). Bone is weakest in tension and strongest in compression (Galloway, 1999; Kroman and Symes, 2013). Angulation is a bending force and is a combination of both tensile and compressive forces. When undergoing bending load, tension will occur on the convex surface and compression will occur on the concave surface. Shearing forces are sliding forces. These tear the bone apart by sliding portions of tissue across each other. Torsion forces (also called twisting

or rotational) cause compression and tension along the longitudinal axis and shear in the transverse axis (Galloway, 1999).

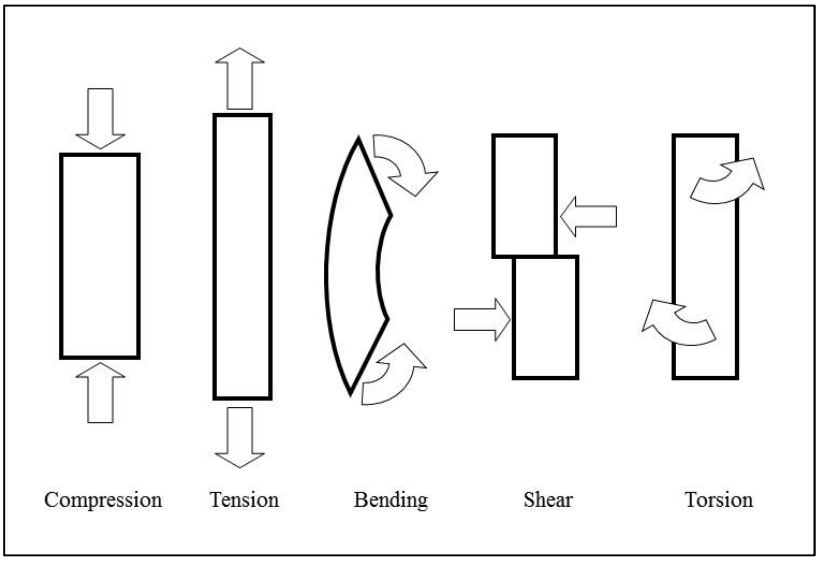

Figure 1.1. Classification of forces acting on bone. Arrows indicate the direction of force.

The numerous classifications of fracture types depend on the type, amount, and location of the force applied, the degree of fracturing, and the type of bone. For this study only complete fractures are relevant and thus included here (Figure 1.2). Transverse fractures are fractures that run perpendicular to the long axis of the bone and occur as right angles to the long axis of the bone. These are often caused by three-point bending, when a blunt object imparts severe angulation; however, bones are not necessarily under compression from normal weight-bearing functions at the time of fracture (Galloway, 1999). Oblique fractures usually occur at a 45 degree angle across the diaphysis due to shear forces (Evans, 1973). Similar to transverse fractures, they are created when

angulation force is applied to a bone, although there is also compressive force placed on the ends of the bone as well. Spiral fractures are often created by rotational forces on the bone that cause a tensile shear failure. The fractures begin as small cracks that propagate around the bone by following the peak of the tensile loading (Galloway, 1999). Comminuted fractures occur when more than two fragments of bone are created, which usually involves relatively high levels of force (Gonza, 1982).

For this study it is most important to understand angular or bending forces. In angulation the ends of the bone are stabilized while a force is applied to a central point. Due to its structure, bone initially bends around the point of impact, which creates a concave surface (inside curve) on the side of the impact and a convex surface (outside curve) opposite of the point of impact. This subjects the bone to tensile forces on the convex surface and compressive forces on the concave surface (Ubelaker and Adams, 1995; Galloway, 1999; Kroman and Symes, 2013). Since bone has greater resistance to compression than to tension, failure will initially occur at the area of tension. The fracture will then radiate back to the compression side of the bone. As the fracture propagates it will travel along the shear plane in both directions creating a triangular-shaped wedge of bone on the concave side. This specific type of fracture is commonly referred to as a butterfly or wedge fracture (Gonza, 1982; Ubelaker and Adams, 1995).

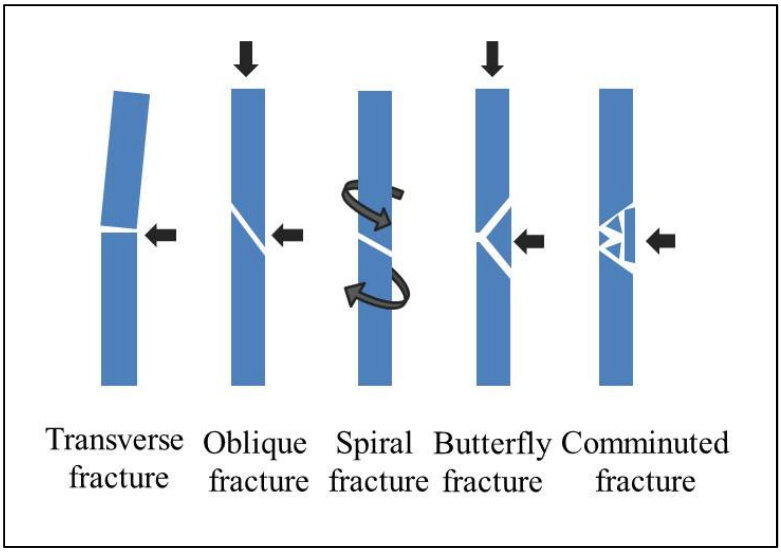

Figure 1.2. Classification of fracture types. Arrows indicate the direction of force.

As previously mentioned, the microstructure of bone is an important determinant in fracture initiation and propagation. Osteons contribute to the toughness and fatigue strength of bones through osteonal debonding and pullout (Hiller et al., 2003). When cortical bone is placed under tension, osteons debond from the interstitial matrix and "pull-out" in order to reduce the strain and control the fracture proliferation by bridging the advancing crack (Figure 1.3). Hiller and colleagues (2003) assert that pullout occurs when the tensile strength of an osteon exceeds the shear strength at its cement line. When the deformation becomes too great and failure begins along the cement line (Evans, 1973), the portion of the bone under tension will have its osteons pulled out of the fracture surface in a telescoping fashion. Conversely, on the compression side of the fracture, there is no osteon pullout. Thus, Hiller and colleagues (2003) found that the microsurface of the fracture is markedly variable depending which forces are applied. Tensile force causes osteonal pullout that produces textured and rough fracture surfaces,

whereas compressive force does not cause osteonal pullout and therefore does not produce rough fracture surfaces.

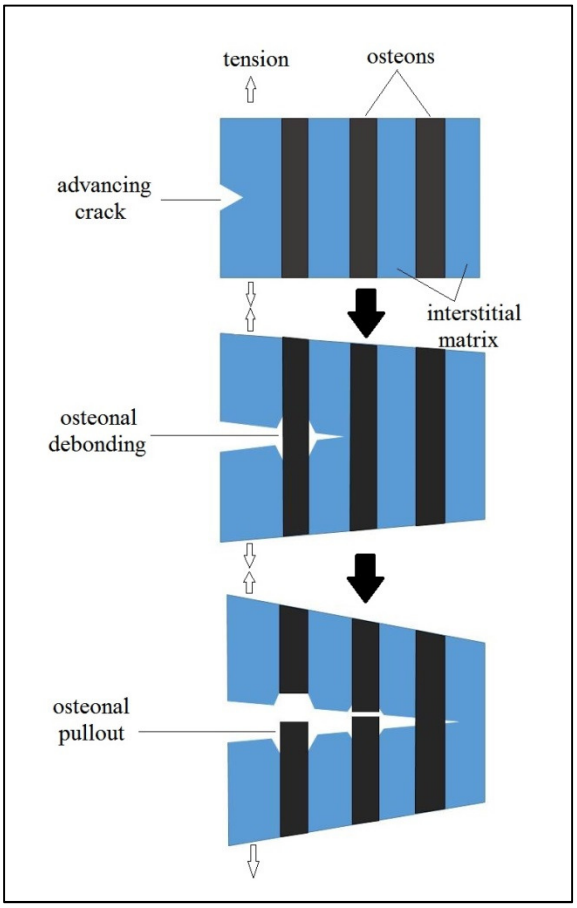

Figure 1.3. Schematic diagram illustrating osteonal pullout. Tensile loads produce a crack that cuts across osteons in the interstitial matrix. Osteons debond from the matrix and bridge the gap until failure occurs. When the osteons fail at sites above or below the crack surface they produce pits and projections, which produce irregular fracture surface morphology. (Adapted from Hiller et al., 2003)

The Timing of Fractures

Antemortem fractures occur while the individual is still alive and can usually be determined based on the presence of an osteogenic reaction (Sauer, 1998). Evidence of

healing, absorption, or infection is indicative of antemortem injury. One of the first signs of healing is the rounding or remodeling of the fracture edges (Aufderheide and Rodriguez-Martin, 1998; Sauer, 1998), although these are often difficult to detect within the first week of initial injury (Maples, 1986; Galloway, 1999).

Perimortem fractures occur around the time of death and will exhibit green fracture characteristics without any signs of healing or osteogenic reaction (Johnson, 1985; Sauer, 1998). In contrast, postmortem damage occurs after death and is usually identifiable because the bone will exhibit dry bone fracture characteristics rather than fresh bone characteristics. Postmortem damage often results from scavenging, weathering, or discovery and excavation mishaps (Johnson, 1985; Maples, 1986; Ubelaker and Adams, 1995; Sauer, 1998).

Many authors have noted that the distinction between perimortem and postmortem fractures is largely shaped by the qualities of the bone tissue rather than the timing of the injury (Ubelaker and Adams, 1995; Galloway et al., 1999; Moraitis and Spiliopoulou, 2006; Wieberg and Wescott, 2008). Assessment of perimortem and postmortem fractures are often based on whether the bone was wet or dry at the time of fracture. Living bones retain collagen and moisture and are referred to as “green” or “fresh.” After death, bones begin to lose their organic components, which results in “dry” bone (Johnson, 1985; Ubelaker and Adams, 1995; Sauer, 1998; Wieberg and Wescott, 2008). Wet and dry bones have different responses to forces because wet bone is more ductile while dry bone is more brittle. Wet bone has high collagen and moisture content that make it ductile and resistant to tensile stress; it is able to undergo more plastic deformation before fracturing than dry bone. Decomposition dries out bone and degrades

the collagen so that the elasticity is lost and it becomes brittle (Johnson, 1985; Maples, 1986; Sauer, 1998; Galloway et al., 1999).

Since wet and dry bones have different mechanical properties, assessment of the fracture characteristics can help provide clues to the timing of the fracture. In addition, color variation may also help distinguish between perimortem and postmortem fractures. Therefore, there are three characteristics are typically used to distinguish between perimortem and postmortem fractures: color differences, macroscopic fracture morphology (including fracture outline, surface, and angle), and microscopic fracture morphology (Galloway et al., 1999; Moraitis and Spiliopoulou, 2006; Wieberg and Wescott, 2008).

Bones may be stained by hemorrhage, decomposition fluids, or by postmortem contaminants such as soil or dirty water (Maples, 1986; Moraitis and Spiliopoulou, 2006; Wieberg and Wescott, 2008). Anthropologists can assess when the fracture occurred by comparing the color of the fracture surface to the color of the external bone surface. If the exposed fracture surface is the same color as the external cortical surface, then the fracture may be assumed to have occurred before the postmortem period. On the other hand, if the two surfaces are different colors (i.e. the fracture surface is lighter), it is likely that some postmortem damage occurred (Johnson, 1985; Galloway et al., 1999; Wieberg and Wescott, 2008).

Certain types of fractures are more commonly seen in perimortem or postmortem fracturing events. The most common fractures to fresh bone are usually characterized as spiral, oblique, or circular in nature (Galloway, 1999). Wet fractures also have distinct patterns of fracture lines that are not seen in dry bone, such as radiating fractures and

concentric circular fractures of the cranium (Johnson, 1985; Maples, 1986). In addition, wet bone tends to splinter under force, which often results in "greenstick" fractures that are incomplete with irregular surfaces and edges (Maples, 1986; Sauer, 1998; Galloway, 1999; Wieberg and Wescott, 2008). Butterfly fractures are also common features of perimortem bone injuries, although Ubelaker and Adams (1995) found that butterfly fractures may be produced up to a year postmortem.

In contrast, fractures to dry bone often result in longitudinal and perpendicular breaks. These fractures may also extend into the epiphyses, as the dried trabecular bone is no longer spongy and thus cannot absorb the stress (Johnson, 1985). Dried bone is more brittle and is more likely to shatter into small, regular fragments. As drying continues, fragments will become smaller (Maples, 1986).

The fracture outline, defined here as the angle formed by the fracture relative to the long axis of the bone, is dependent on the quality of the bone at time of fracturing. Fresh bones have breakage outlines that are curved or form acute and obtuse angles (i.e. spiral, oblique, and butterfly fractures). Dry bone, in contrast, produces fracture outlines that form right angles to the long axis of the bone or are parallel to the long axis of the bone (i.e. longitudinal and transverse fractures) (Villa and Mahieu, 1991).

Other fracture characteristics commonly used by forensic anthropologists to distinguish perimortem trauma from postmortem damage are fracture angle and fracture edge. The fracture angle is the angle formed by the fracture surface and the outer surface of the cortical bone. Fresh bone fractures commonly present acute and obtuse angles, whereas dry bone tends to break perpendicular to the outer cortical surface at a right angle (Johnson, 1985; Villa and Mahieu, 1991). Fracture edge, the morphology of the

fracture margin, may also be used to differentiate wet and dry bone fractures. Green bone exhibits smooth or sharp fracture edge, while dry bone displays irregular to jagged, but blunt, fracture edges (Johnson, 1985; Villa and Mahieu, 1991; Ubelaker and Adams, 1995).

Fracture surface may also change with the quality of the bone tissue. The fracture surface is defined as the cross-sectional area of cortical bone exposed by the complete fracture (Johnson, 1985). Fresh bone fractures will have a smooth fracture surface texture, whereas dry bone will exhibit a rough, jagged fracture surface (Johnson, 1985; Villa and Mahieu, 1991). Stepping and hackle marks are fracture surface features that may be seen in certain types of bone breaks. Stepping occurs when dehydrated, weathered bone cracks parallel to its longitudinal axis. When the fracture propagates across the bone, the fracture front jumps to the cracks and terminates. This creates a stepped edge or right angle offset that is frequently seen in dry bone fractures (Johnson, 1985; Bonnichsen and Will, 1980). Hackle marks occasionally occur on the fracture surface of fresh bone breaks. These marks are discontinuous curved ridges that are found in shear failure and run parallel to the propagation of the fracture (Johnson, 1985).

Finally, there are microscopic differences in the fracture surfaces of perimortem and postmortem bone fractures. Using scanning electron microscopy (SEM), Shipman (1981) found that perimortem fracture surfaces appear roughened or string-like microscopically. This is in contrast to the even, fine-textured macroscopic fracture surface that Johnson (1985) describes. Shipman (1981) postulates that the string-like microscopic surface is due to adjacent collagen bundles being torn apart during the fracturing process. It is also possible that the osteonal pull-out that Hiller and colleagues

(2003) describe (Figure 1.3) may also contribute to the rough, string-like fracture surface. However, both the macroscopic and microscopic examination of dry bone fracture surfaces describe the surface as roughened and stepped. This is due to the fracture front running perpendicular to the collagen fiber bundles (Shipman, 1981; Johnson, 1985; Wieberg and Wescott, 2008).

Perimortem and postmortem bone fractures may be differentiated with evaluation of color changes, macroscopic fracture morphology, and microscopic fracture morphology. As demonstrated above, the determination of perimortem trauma or postmortem damage is largely based on if the bone was wet or dry at time of fracturing. Since the loss of moisture and organic components are dependent upon a number of environmental factors, bones can retain their moisture and collagen fiber matrix well after death, depending on the depositional environment (Maples, 1986; Wieberg and Wescott, 2008). Indeed, Maples (1986) noted that bones can retain their elasticity for several weeks after death, during which time they continue to exhibit perimortem fracture characteristics. It remains unknown at what point fresh bone changes to dry bone, as wet and dry are points along a continuum and distinction between the two is subjective (Johnson, 1985). Thus, although fractures to wet and dry bone have distinctive characteristics, distinguishing between perimortem and postmortem fractures is problematic because the transition from wet to dry is ambiguous (Sauer 1998; Galloway et al., 1999; Wieberg and Wescott, 2008).

Establishing a Perimortem Interval

There have been many recent studies investigating bone weathering and long bone fracture characteristics in the perimortem and postmortem intervals. The purpose of these studies is to better understand the temporal limits of the perimortem interval, especially in different environments, as weathering rates of bones differ by climate (Behrensmeyer, 1978). These studies also focus on how bone weathering or drying can affect the way blunt force trauma manifests on the skeleton throughout the perimortem and postmortem intervals.

Bell and colleagues (1996) examined postmortem changes to skeletal remains to determine the speed at which the microstructure of the bone changes. The authors found that the depositional environment (e.g. waterlogged bog, intertidal salt water, surface air-exposed) greatly contributed to the microstructural and morphological changes that appeared. In addition, they confirmed that postmortem alteration of bone could occur less than three months after death (Bell et al., 1996). In a study of bone weathering in Southern Ontario, Janjua and Rogers (2008) observed that defleshed pig bones did not exhibit significant cortical drying until after about nine months of outdoor exposure. These two studies exemplify the variability of bone decomposition and drying when exposed to different environments and other taphonomic factors. Therefore, as a result of these diverse decomposition rates, the length of time that bones exhibit wet fracture characteristics is affected by depositional environment.

Wheatley (2008) examined the relationship between weathering and bone fracture characteristics in Central Alabama. The purpose of this investigation was to test and quantify the characteristics commonly used by forensic anthropologists to determine the

timing of the fracturing event. Results of this study show that there are significant differences in fracture characteristics manifested by fresh and dry bones. However, despite these statistically significant findings, the author asserted that the fracture attributes were not reliable enough to differentiate between perimortem and postmortem fractures in a forensic investigation (Wheatley, 2008).

In a related study, Wieberg and Wescott (2008) focused on the relationship between bone moisture content, fracture characteristics, and the postmortem interval. They obtained sixty pig bones and fractured them every 28 days (starting at PMI=0) for five months in Central Missouri to examine the monthly changes in bone moisture content and fracture morphologies (outline, angle, and surface). They found that the moisture content of bones decreases significantly and rapidly during the first two months postmortem, but after the first two months the drying process slows down. Fresh fractures generally presented smooth surfaces, obtuse and acute angles, and curved or "v" outlines, whereas later fractures had jagged surfaces, right angles, and fewer curved or "v" outlines. These results coincide with previous literature on fracture morphologies, although they found that fracture angle had the most inconsistent relationship with PMI. Overall, Wieberg and Wescott (2008) observed that bones retain "fresh" properties well into the postmortem interval, and that bones did not consistently exhibit postmortem characteristics until after five months in Central Missouri during the summer.

Similar to Wieberg and Wescott (2008), Shattuck (2010) assessed perimortem changes in long bone fracture characteristics, although her study took place in the climate of Southwest Texas rather than Central Missouri. Aside from the assessment of the differences between perimortem and postmortem fracture characteristics, this study

endeavored to establish a possible time frame for the transition from wet to dry bone. Fifty pig long bones were exposed to natural taphonomic conditions and broken every two weeks over a 128-day period, and the fracture patterns, angles, and edges were then evaluated. Fracture surfaces tended to change over time from smooth to jagged, and there was an increased incidence of transverse fractures as the postmortem interval increased. All bones fractured during the first two weeks exhibited entirely smooth fracture surfaces, and those fractured at least ten weeks after death exhibited exclusively jagged fracture surfaces. Overall, no bones exhibited purely postmortem fracture characteristics by the end of the 128-day period.

My research attempts to develop a novel method for distinguishing between perimortem and postmortem blunt force trauma fractures in long bones. While previous research (e.g. Johnson, 1985; Villa and Mahieu, 1991; Wieberg and Wescott, 2008; Shattuck, 2010) has established that fracture surface morphology changes throughout the postmortem interval, no studies have made attempts to calibrate or measure these changes. The current study endeavors to be the first to do so by utilizing GIS technologies and spatial analytical methods. Due to the findings of Hiller and colleagues (2003), the focus of this study is only on the tension fracture surface because osteonal pullout differentially affects the morphology of the tension and compression sides of the fracture surfaces.

CHAPTER II

Materials and Methods

In this study, porcine bones, which have served as a substitute for human bones in a variety of trauma research (Sauer, 1998; Tucker et al., 2001; Wieberg and Wescott, 2008), are used as a proxy for human skeletal remains. The sample is drawn from a collection of over 200 porcine long bones (hereafter referred to as the Forensic Anthropology Center at Texas State (FACTS) collection) with blunt force trauma generated from the time since death to approximately one year after death. The FACTS collection, currently housed at the Grady Early Forensic Anthropology Laboratory at Texas State University (TXST), is extensively documented and serves as an adequate sample to study in this experiment, and was therefore used for experimentation and analysis rather than conducting new fracture experiments.

The FACTS collection of porcine long bone specimens originates from two separate experimental studies. The first was conducted at the University of Missouri in the summer of 2005 (Weiberg and Wescott, 2008). The authors used sixty long bones from ten pigs (*Sus scrofa*) whose weight ranged from 150-200 pounds. All limbs were collected within eight hours of death, wrapped in plastic bags, placed in paper bags, and frozen until all specimens could be collected. All soft tissue was left intact for this experiment. Once all sixty long bones were obtained, the bones were thawed to room temperature. Ten bones were fractured right away, and the rest were placed on the ground outdoors to simulate the normal decomposition process. Ten bones were fractured every 28 days for 141 days (five months) using a drop impact bone breaking apparatus. This

strike bar, weighing 10.2 kg and dropping from 0.48 m, produced a force of 106 kg/cm^2. Soft tissue was removed for the purposes of clear and thorough examination of the fracture surface, but only after fracturing occurred (Weiberg and Wescott, 2008).

The second portion of the collection comes from a study conducted at the Forensic Anthropology Research Facility (FARF) at TXST. In 2011, Cristina Figueroa-Soto, Maggie McClain, Lauren Springs, and Caryn Tegtmeyer used approximately 158 domestic pig (*Sus scrofa*) long bones for their research project "Broken Bones: Examining Blunt Force Trauma Characteristics Throughout the Postmortem Interval" in which they studied postmortem fracture patterns in south-central Texas (unpublished manuscript). The authors adopted the methods for their study from Weiberg and Wescott (2008) and Shattuck (2010), so much of their research design followed similar guidelines. Rebecca Shattuck (2010) used approximately fifty domestic pig (*Sus scrofa*) femora for her thesis research in which she studied perimortem fracture patterns in south-central Texas. Unfortunately, the specimens from Shattuck's (2010) study were unavailable for use in this current research project and are not currently part of the FACTS collection of porcine long bone specimens.

For their 2011 research project, Figueroa-Soto and colleagues used pigs weighing between 200-250 pounds and collected the long bones within 24 hours of death. They then froze the bones in plastic and paper bags until all 158 could be obtained. Unlike Weiberg and Wescott (2008), however, the authors chose to use defleshed bones that had only minimal muscle, cartilage, and fat still attached. This was done in order to better simulate the effect of weathering on already skeletonized remains (Shattuck, 2010). After all specimens were collected, the frozen limbs were allowed to thaw until they reached

room temperature. Four bones were immediately broken and the rest were placed outdoors at FARF and allowed to dry naturally. The authors fractured four bones every seven days for a period of 273 days (ten months) using a drop impact bone breaking apparatus. This strike bar was made of galvanized steel, weighed 6.4 kg, and was dropped from 1.48 m onto the bone. This produced a force of 10,920.66 kg/m^2 (Shattuck, 2010). Access to all of the bones has been granted by the original investigators.

In this study, a total of eighty long bones from the FACTS collection were used. While attempts were made to use specimens from each PMI and to have relatively equal sample sizes for each PMI, in some cases the bones were too fragmentary or otherwise damaged to be used. No fibulae from the collection were used because pig fibulae are very small in diameter, and analysis on such a small fracture surface would not be feasible with the present scanning technology. An additional five specimens were not considered for analysis because the radius and ulna had fused. In adult pigs, the radius and ulna naturally fuse together (Adams and Crabtree, 2012); this phenomenon, however, affects how the bone(s) respond to force, and since this fusion does not happen in humans, these specimens were excluded from analysis. Finally, it is important to note that of the 158 specimens originating from the FARF portion of the FACTS collection, 14 were missing and 12 had no apparent fracture. Therefore, due to restricting criteria and other problems associated with fragmentation, only eighty of the possible 218 specimens in the FACTS collection were used in this study. When possible, both sides of the bone were scanned, but this was not always feasible. A total of 144 scans were used for analysis.

NextEngine© Scanner

With technology continually advancing, surface scanning has become a convenient tool for anthropologists. One of the most important benefits of surface scanning is its non-invasive, non-destructive nature that allows for specimen conservation. Other benefits of surface scanners are that they provide rapid generation of dense 3-dimensional meshes, have very high resolution, and are affordable (Friess, 2012).

For this project, a NextEngine© 3D laser scanner (NextEngine, 2011) was used to scan the fracture surface of selected bones in the FACTS collection of broken pig long bones. The scanner uses High Definition laser precision to capture the size, shape, texture, and color of the object, and the included ScanStudio© software builds a 3D mesh model using these variables. This mesh model can be used for 3D printing, computer-generated imagery (CGI), or conversion to computer-aided design (CAD). The scanner is accurate up to 0.127 millimeters (mm) and captures about 16 points per millimeter (NextEngine, 2011).

According to Friess (2012), models of hard-tissue anthropological objects (bones) created with surface scanners are sufficiently precise. In terms of anthropometric measurements, the differences between a scanned model and the original are comparable to the standard allowable errors in anthropometry. Slizewski and colleagues (2010:186) compared various surface scanners and found that in small and medium-sized bones, a NextEngine© scanner provides a "good level of details and accuracy" and creates a high quality external surface of the bone.

The cost of a scanner is generally correlated with the quality of optics and the software that operates the scanner, rather than with resolution (Friess, 2012). Thus, a low-

cost scanner like the NextEngine© (~$3,000) may produce a model that is just as accurate as a mid-range scanner ($20-50,000). Indeed, after comparing the precision of three different scanners, Guidi and colleagues (2007) encouraged users to choose a scanning device based on affordability.

Scanning Process

All specimens used in this analysis were completely fractured into two or more pieces. Since a complete fracture results in two or more fragments of bone, each specimen generally had two scans associated with it: one scan of the fracture surface on the proximal shaft and one of the fracture surface on the distal portion of the shaft. This often resulted in two scans per single fractured specimen. However, only the fractured surfaces that were part of the larger distal or proximal shaft were chosen for scanning; fragments such as "butterfly" fragments were not scanned.

Before scanning a specimen, the tension and compression portions of the break were identified by piecing the fractured ends of the bones together. The areas of tension were marked with a pencil so that the scanner, scanning in color, would include the pencil marks onto the scanned model of the bone. This made editing the scans easier and more precise because the tension portion of the fracture surface was easily demarcated on the digital model.

The desktop setup consisted of the computer, the scanner, and the multidrive, a two-axis positioning turntable that creates complete scans of small objects (Figure 2.1). The first axis rotates the object 360° and the second axis tilts the object from -35° to +45° (NextEngine, 2011). This two-axis model allows the top and bottom of the object to be

scanned at the same time that the sides are scanned, and the software automatically aligns and merges these acquired images. This reduces the amount of time the user spends processing the scan images. The multidrive is connected to the scanner, which has two sets of four lasers: one set is used for macro mode and the other set is used for wide mode (NextEngine, 2011). Because the bone fracture surface only measures as large as the circumference of the bone, the macro mode was used to scan a close-up view of the fracture surface.

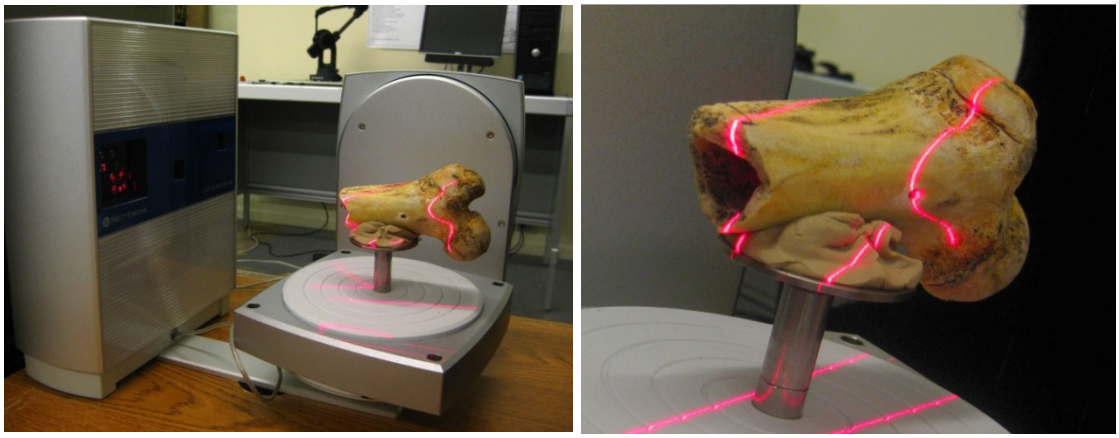

Figure 2.1. The NextEngine© scanner. View of the set up of the scanner (left), and close up of the longbone being scanned (right).

Each bone was adhered to the multidrive using putty: the bone was placed length-wise across the platform, the fractured side facing the scanner, and putty was used underneath and around the sides to secure the bone in place. A piece of black velvet photography cloth was then placed behind the multidrive. This cloth served the purpose

of absorbing the lasers, as well as preventing the lasers from picking up background objects.

NextEngine© offers many options and features for scanning objects. The software can create a full 360° scan, a bracket 180° scan, or a single, two-dimensional scan. Due to the fact that only the ends of the fractured shafts were under analysis, bracket scans were chosen. Each scan used 12 divisions (angles) to capture the fracture surface, and a neutral object color was selected to represent the color of the bone. The highest resolution, 40,000 points/in^2, was used in order to provide the best possible representation of the fracture surface. These settings remained constant for all scans.

The benefit of the multidrive is that it has the option of performing up to five scans of the same object at different user-defined angles. This "scan family" allows the user to choose the angles that will best capture the texture of the scanned surface, and then the software automatically aligns the scans together to form one mesh object. Since each fracture surface is different, the start and tilt settings of the multidrive changed for each specimen. A scan takes approximately 30 minutes to complete.

Editing the Scans

After scanning each specimen, the mesh model of the bone was readied for analysis. In general, the post-processing of a 3D model consists of aligning multiple single-dimension scans into one 3D model, trimming away any unwanted data, and fusing the scans into one mesh object (Figure 2.2). Since the ScanStudio© software automatically aligns the scans, the alignment step of scan editing was not needed. Thus, the first phase of scan editing was to trim the scans down until only the tension portion of

the fracture surface remained. This step eliminated areas of the scan that were not needed for analysis, such as the trabecular bone inside the medullary cavity. Trimming was made easier by the high resolution of the scanner; it was possible to zoom in on each scan to a fraction of a millimeter, find the edges of the tension fracture surface, and then trim away any unwanted data. If it was difficult to discern the exact outline of a tension fracture surface because of the fracture or bone morphology, the scan was trimmed more conservatively to ensure that only the tension surface remained.

After trimming, the scans needed to be fused into one mesh model (Figure 2.3). When the software aligns a group of scans together it simply overlays multiple scans on top of each other. Fusion takes these scans and merges them so that there is one final assembled scan. Fusion allows for decimation, a "process by which the total number of polygons in a mesh is reduced while the original geometry is preserved as much as possible" (Friess, 2012:5). No decimation (i.e. simplification) was used in this project so that the original fracture surface was preserved.

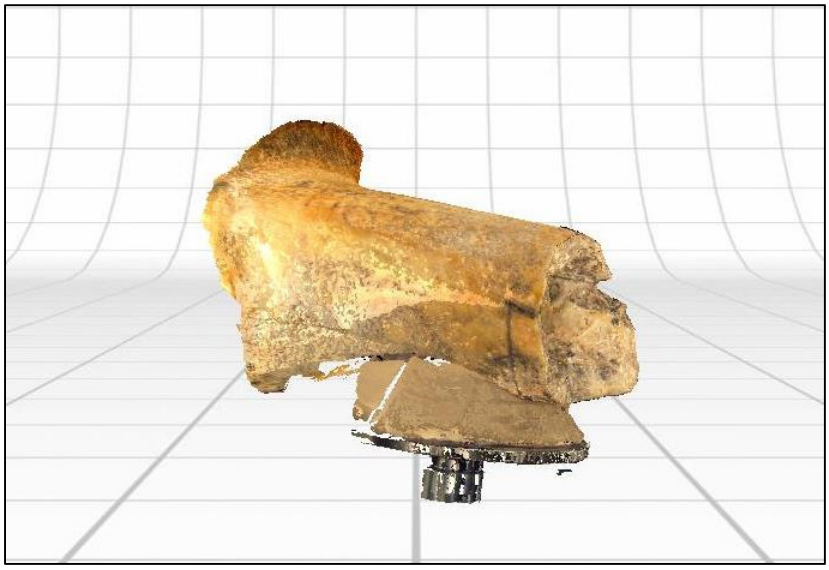

Figure 2.2. Output of a completed model in NextEngine©. Note that this specimen had not yet been trimmed down to just the fracture surface for analysis.

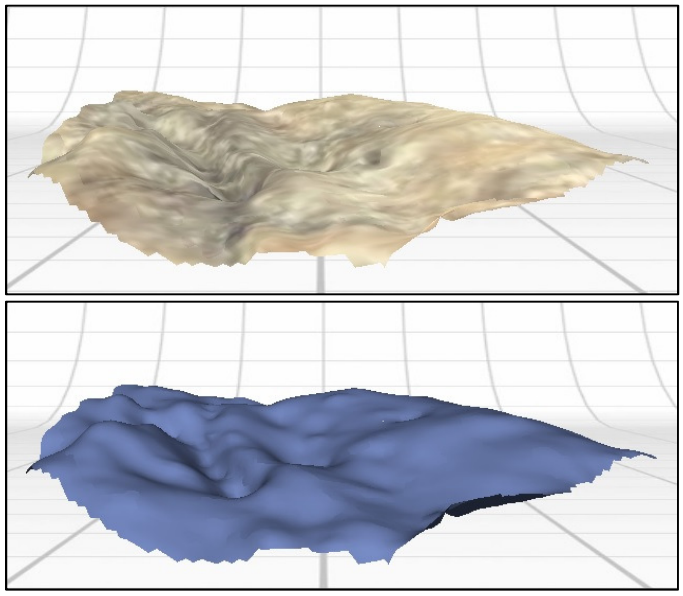

Figure 2.3. Completed scan (aligned, trimmed, fused) for analysis. The same scan is shown in color (top) and shaded (bottom) to depict the "landscape" of the fracture surface.

The final processing step before analysis was to orient the model using CAD tools. The purpose of this step was to position the fracture surface in a transverse plane, perpendicular to the sightline of the viewer, so that it mimics the way a satellite looks directly down at the Earth (Figure 2.4). By orienting the model in such a fashion, the elevation points on fracture surface have a standardized reference plane. After orienting the model, the scan was exported as a series of X, Y, and Z coordinate points into ArcGIS©, a Geographic Information Systems (GIS) software program. The .xyz file type is the only file output of the ScanStudio© software that is compatible with GIS.

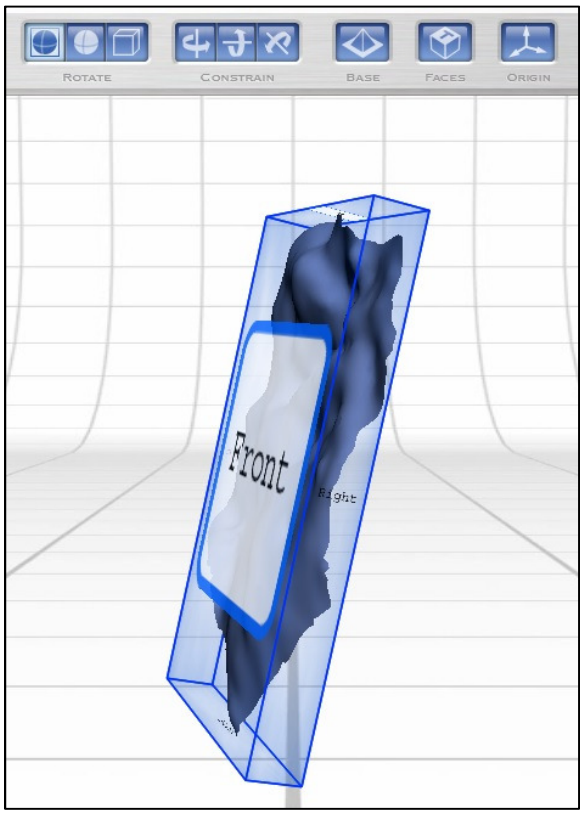

Figure 2.4. Orienting the fracture surface using CAD tools. The scan shown is at an angle to better illustrate the process of orientation.

Geographic Information Systems

Geographic Information Systems (GIS) is a technology that can be used to "support both science and problem solving….a tool for revealing what is otherwise invisible in geographic information…" (Longley et al., 2005:16). Geographic Information Systems software is designed to analyze spatial data associated with specific points on the surface of the Earth (Longley et al., 2005). The GIS software program ArcGIS© was used to examine the 3D scans of the fracture surfaces with spatial statistics. Conceptually, the irregular landscape of a fracture surface is akin to the Earth's landscape, so using GIS to analyze fracture surfaces is a new application of the technology. The collagen fiber bundles and osteon pullouts that form the fracture surface create hills and valleys that GIS can produce visual models of and analyze.

The coordinate points of each scan were imported into ArcGIS© and a new feature class (map layer) was created to represent each unique fracture surface. The resulting fracture surface was illustrated by thousands of individual points (Figure 2.5). This type of data structure is called vector, meaning that it is in the form of discrete points, lines, or polygons that are represented by exact X and Y coordinates rather than pixels (DeMers, 2009).

It is important to note the interaction between scale and resolution in GIS. The larger the scale is, the higher the resolution will be. As the scale decreases, resolution is lost and boundaries may become more generalized or simplified (DeMers, 2009). As a result, the interpretations of a map will change as the level of the map scale will changes. For example, a river basin shown on a map at two different scales, one higher and one

lower, means that the resolution of the river basin is different for each scale. The larger scale allows for finer resolution of the river basin that shows many more flow lines, and the smaller scale has lower resolution but the major flow lines are still present. A smaller scale may be better suited to point out generalizations in the data, whereas a larger scale may be better suited for more specific detail. Thus, different scales and resolutions could answer different questions about the data. The data from this study are at a very large scale and high resolution, which is evidenced by the thousands of data points that are represented on a fracture surface measuring only centimeters in length.

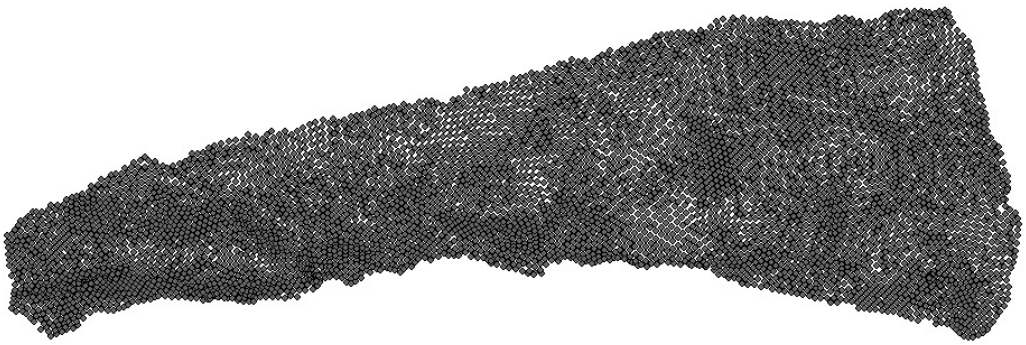

Figure 2.5. PMI 0, Specimen #1, Side 2. Approximately 6,733 individual points are plotted to represent the fracture surface.

In this study, the hot spot analysis tool within the ArcGIS© Spatial Statistics toolbox was used to identify clusters and patterns on the fracture surfaces. In spatial analysis, hot spots are areas within cities or other geographic locations where there is a significant clustering of crime incidents. The hot spot analysis tool identifies statistically

significant areas of hot spots (high crime) and cold spots (low crime) for a specific geographic location. It also provides visual representation of clusters and their extent (Levine, 2013). This study adapted this tool to identify clusters of high and low elevations (i.e. areas of hills and valleys) rather than clusters of high and low crime incidents.

The hot spot analysis tool uses the Getis-Ord Gi* statistic to recognize statistically significant spatial clusters of features that have similar levels of a specified attribute (Levine, 2013). The attribute of interest for this analysis is Z, the elevation point associated with an X,Y coordinate point. The Getis-Ord Gi* statistic is a measurement of spatial autocorrelation. Spatial autocorrelation is a concept that indicates a non-random arrangement of incidents and implies that a lack of spatial independence exists (Levine, 2013). In other words, spatial autocorrelation implies that pairs of subjects that are spatially close to each other are likely to be more similar than pairs of subjects that are farther away from each other. Thus, hotspot analysis of the fracture surfaces identified clusters of high and low elevation (Z) values and assessed whether those clusters were statistically significant within the context of neighboring feature values.

Running the hot spot analysis tool requires choosing an input feature class, input feature, and threshold distance. The input feature class is the fracture surface. The input feature is Z, the elevation for each point. The threshold distance is a sphere of influence that surrounds any given feature (in this case, a coordinate point). Each feature is analyzed within the context of the neighboring features that fall within this sphere of influence, and each of these neighbors is given an equal weight. The default setting for threshold distance may be used, or the user may define a custom threshold distance.

Unfortunately, the default setting changes for each fracture surface under analysis. Thus, for the purposes of consistency and replication, the threshold distance for each analysis was customized and defined as 1% of the total length of the fracture surface. The 1% threshold distance was chosen because of the results of a sensitivity analysis testing 10%, 5%, 1%, and 0.5% of the total fracture surface length. The sensitivity analysis found that using 1% of the fracture surface length as the threshold distance yielded results most similar to the output of the default threshold distance. The customized ratio for each fracture surface allowed for consistency throughout the analysis.

The output of this tool is a z-score, p-value, and confidence level for each feature. An output feature class (map layer) is created to illustrate the z-scores for each feature, and different confidence levels (90%, 95%, and 99%) are represented on the map with different colors. Very high and very low z-scores with low p-values are represented on the map with deep red and blue hues (Figure 2.6). The map layer also provides a visual depiction of the location and extent of each cluster.

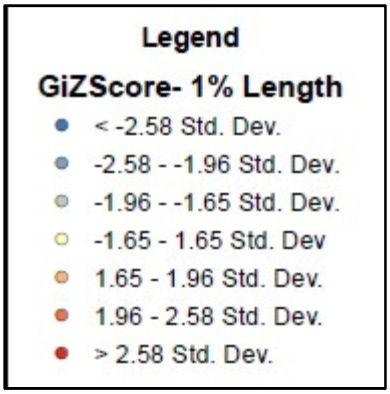

Figure 2.6. Example of the legend for hot spot analysis output. The darkest blue and darkest red indicate points whose elevation is considered significant at the 99% confidence interval. These points are termed hot spots and cold spots. The 1% length refers to the threshold distance chosen for analysis.

Statistical Analysis

Each fracture surface was analyzed using hot spot analysis. This tool was chosen because I expected the locations of osteons to correlate with the hills and valleys on the fracture surface. In other words, low values from osteonal pullout would be near each other and cluster to form valleys, just as high values from osteonal pullout would cluster near each other to form hills. The percentage of the fracture surface that classified as cold spots, hot spots, and intermediate values in the middle of the distribution were recorded for each specimen. Hot and cold spots were clusters of features whose z-scores fell outside the range of the critical values defined by the 99% confidence interval. Intermediate z-scores represent the expected outcome of a random distribution of values and were those z-scores that failed significance at the 90% confidence interval. These values can be considered to be representative of the flat (smooth) areas of the fracture surface.

The average percentage of the fracture area considered hot spots, cold spots, and intermediate values were calculated for each weekly PMI and again for each month. Because of the large sample size, averages helped elucidate any trends in the data at the weekly and monthly levels.

A one-way analysis of variance (ANOVA) test was used to look for correlations between the percentage of cold spots and PMI, the percentage of hot spots and PMI, and percentage of intermediate values and PMI. For most of the statistical analyses, including the ANOVAs, the bones were grouped by PMI in one month intervals. For example, PMI Group I consists of bones broken between 0 and 28 days. For other analyses the bones

were grouped as “green” or less than 2 months PMI, intermediate or 3-6 months PMI, and “dry” or greater than 6 months PMI. Since Wieberg and Wescott (2008) found that the drying process of bone slows down significantly after two months, a t-test was used to look for statistical differences between the first two months and everything after two months.

Finally, regression analysis was used to examine the relationship between percentage of cold spots and PMI, percentage of hot spots and PMI, and the percentage of intermediate (flat) areas and PMI. This analysis looked for the regression that best fit the data and went with linear regression. Specimens were grouped by week, month, and stage of decomposition (early, middle, late).

CHAPTER III

RESULTS

The hot spot analysis tool was used on a total of 144 scans to generate map layers and attribute tables of values for each fracture surface. The attribute table included all of the original elevation values and the calculated z-scores and p-values for each data point (Figure 3.1). These values were then plotted by significance of the z-value and illustrated in a map layer. Since there were thousands of points that made up any given fracture surface, and 144 fracture surfaces under analysis, there was a substantial amount of information produced by this analysis.

Results of the hot spot analysis for four of the specimens (#2, 39, 85, and 131) are shown in Figure 3.2. These four specimens are spaced across the postmortem interval (PMI 0, PMI 63, PMI 147, and PMI 231) and were chosen to be representative illustrations of the changes to the fracture surface across time. The general trend in the data suggests that bones broken closer to the time of death have a higher percentage of their area that classifies as hot and cold spots compared to bones broken later in the postmortem interval. This implies that the bones broken near the time of death exhibit a fracture surface with more hills and valleys than bones broken later in the postmortem interval. However, the area considered intermediate elevation (smooth fracture surface), where the z-value is not considered significant at a 90% confidence interval, always outnumbers the area of hot or cold spots. For the majority of specimens, the area of intermediate elevation also outnumbered the *combined* areas of hot and cold spots as well.

Sp39_S2

FID	Shape *	SOURCE_ID	Z	GiZScore	GiPValue
0	Point ZM	0	69.6524	-0.423481	0.671945
1	Point ZM	1	69.687	-0.166395	0.867846
2	Point ZM	2	69.6629	-0.30945	0.756979
3	Point ZM	3	69.6939	-0.070048	0.944155
4	Point ZM	4	69.2926	-3.596765	0.000322
5	Point ZM	5	69.2834	-3.031099	0.002437
6	Point ZM	6	69.2939	-4.201502	0.000027
7	Point ZM	7	69.3032	-3.705422	0.000211
8	Point ZM	8	69.3284	-3.129557	0.001751
9	Point ZM	9	69.7572	0.45505	0.649073
10	Point ZM	10	69.2735	-4.057622	0.00005
11	Point ZM	11	69.2891	-3.854339	0.000116
12	Point ZM	12	69.3093	-3.468602	0.000523
13	Point ZM	13	69.3093	-3.117172	0.001826
14	Point ZM	14	69.3384	-3.353788	0.000797
15	Point ZM	15	69.3569	-3.606962	0.00031
16	Point ZM	16	69.7561	0.594358	0.552272
17	Point ZM	17	69.7755	0.586052	0.557841
18	Point ZM	18	69.337	-3.182479	0.00146
19	Point ZM	19	69.3745	-3.512245	0.000444
20	Point ZM	20	69.3937	-3.3146	0.000918
21	Point ZM	21	69.7776	0.726179	0.467729
22	Point ZM	22	69.5555	-1.292832	0.196069
23	Point ZM	23	69.5234	-1.206019	0.22781
24	Point ZM	24	69.5583	-1.153947	0.248522
25	Point ZM	25	69.5271	-1.690162	0.090997
26	Point ZM	26	69.4995	-1.682321	0.092507
27	Point ZM	27	69.5263	-1.184906	0.236055
28	Point ZM	28	69.5019	-1.563654	0.117899

Figure 3.1. A portion of the attribute table for specimen #39, scan 2. The z-score and P-value are calculated for each elevation point (Z). The first 28 points of 9,359 are shown here.

To gain a better understanding of any trends in the data, the percentage of the fracture surface area that classified as a hot spot, cold spot, or intermediate elevation was averaged out by week and by month. For instance, PMI 0 has ten total specimens whose percentages of fracture surface area classifying as cold spots, intermediate elevation, and hot spots averaged out to be 17.6% cold spot, 48% intermediate, and 17.3% hot spot. The values for each week were then averaged out per month, so that Month 1= the average of PMI 0-28, Month 2= the average of PMI 35-56, etc. This ultimately reduced the sample

size from 144 to ten, but allowed for basic trends in the data to be seen (Table 3.1). A scatterplot showing the result of the weekly averaged values is available in Figure 3.3, and a scatterplot showing the result of the monthly averaged values is available in Figure 3.4.

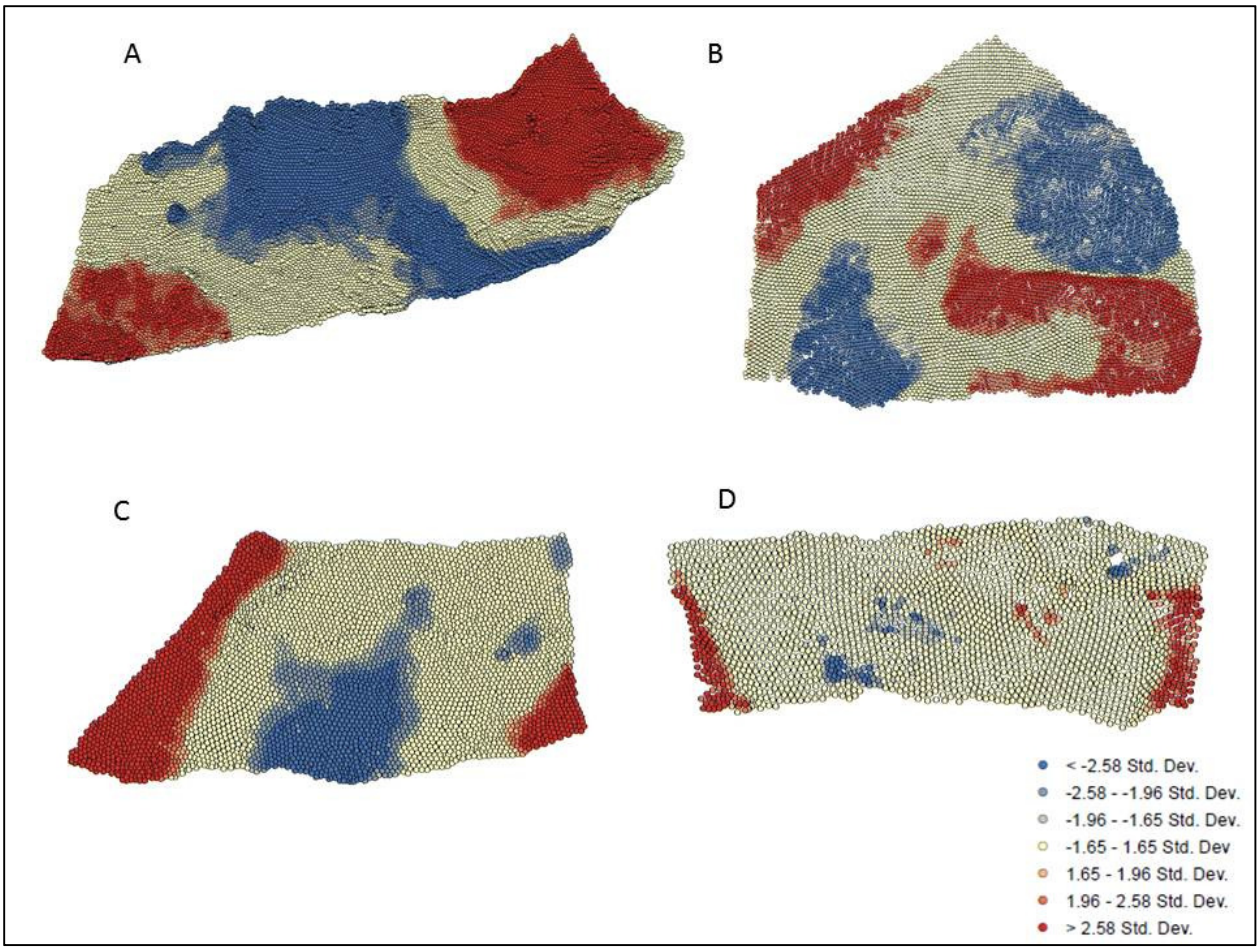

Figure 3.2. Results of the hotspot analysis for four specimens. (A) Specimen #2, PMI 0; (B) Specimen #39, PMI 63; (C) Specimen #85, PMI 147; and (D) Specimen #131, PMI 231. The areas of darkest red are hot spots, the areas of darkest blue are cold spots, and intermediate values are in gray. Notice that from (A) PMI 0 to (D) PMI 231 (9 Months) that the fracture surfaces begin to show smaller areas of hot and cold spots and more intermediate values.

Table 3.1. Monthly averages. Percentage of the fracture surface area classified as cold spots, intermediate values, and hot spots, averaged by month.

PMI (Month)	1	2	3	4	5	6	7	8	9	10
Cold Spots	13.71%	12.29%	13.07%	8.07%	9.64%	12.25%	11.63%	6.44%	8.58%	6.98%
Intermediate	56.77%	58.85%	54.46%	68.27%	65.94%	58.03%	59.01%	71.84%	68.52%	70.76%
Hot Spots	13.84%	12.77%	12.53%	8.18%	7.12%	12.31%	11.48%	6.73%	7.73%	8.08%

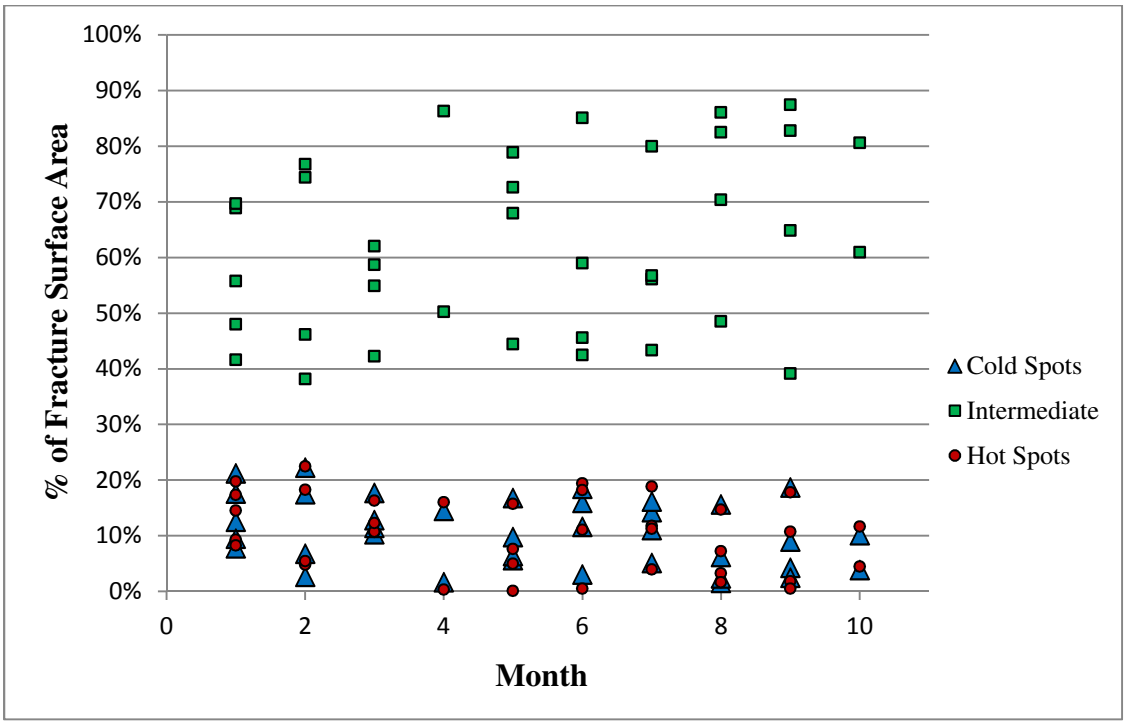

Figure 3.3 Plot illustrating the weekly averages. The percentage of the fracture surface area considered a cold spot, hot spot, or intermediate elevation illustrated by weekly average.

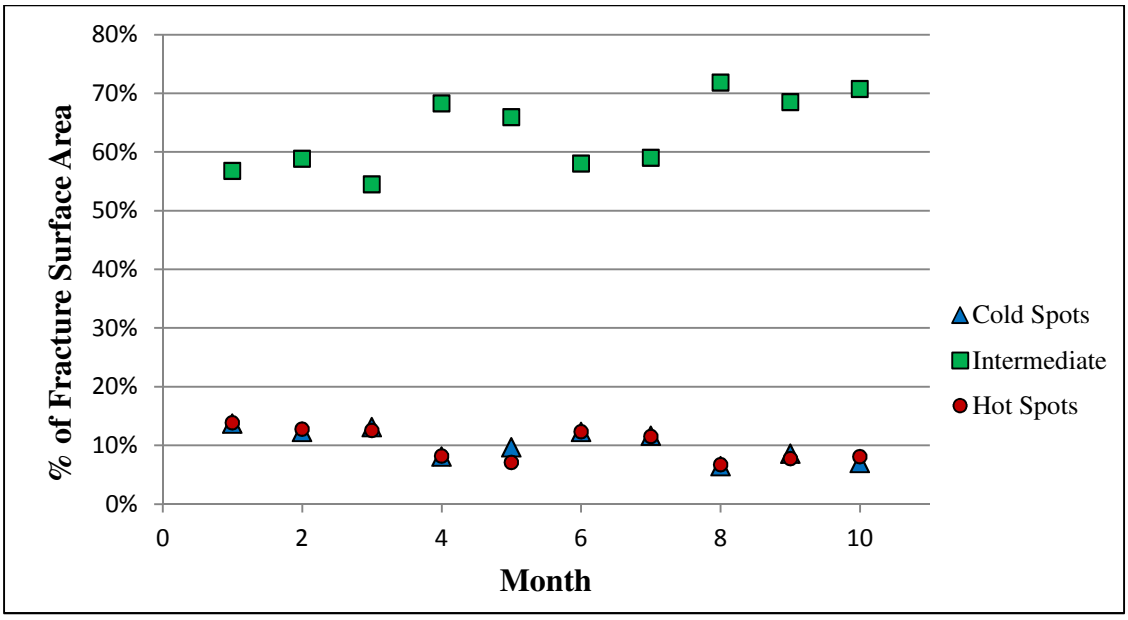

Figure 3.4. Plot illustrating the monthly averages. The percentage of the fracture surface area considered a cold spot, hot spot, or intermediate elevation illustrated by monthly average.

Analysis of variance was conducted to determine if the percentage of the fracture area(s) that are cold spots, intermediate elevation, and hot spots correlated with PMI at monthly intervals. Results indicate that there is no significant correlation between cold spots and PMI (P= 0.099), intermediate elevation and PMI (P= 0.129), or hot spots and PMI (P= 0.124). While none of these are significant, they are approaching significance. When statistical tests were run on larger temporal intervals that corresponded with early, middle, and late decomposition, ANOVA results suggest significant correlations (Table 3.2).

Because Wieberg and Wescott (2008) found that the drying process of bone slows down significantly after two months, t-tests were used to look for statistical differences between the first two months and everything after two months (months 3-10). The t-tests show that there are significant changes in the percentage of the area that are cold spots and the percentage of the area that are hotspots between these two timeframes (Table

3.3). Interestingly, the t-test results for the intermediate elevation do not show significant differences between the first two months and everything after two months. So while the ANOVA found significance for the percentage of area that is intermediate elevation across the early, middle, and late timelines, the t-test found that combining months 3-10 together decreased the variation between the groups and increased the variation within the groups.

Table 3.2. Summary of ANOVA values. Postmortem interval (early, middle, late decomposition) is the primary variable. Early is months 1-2, middle is months 3-6, and late is months 7-10.

	F	*P-value*	*F crit*
Cold Spots	4.658246	0.01099	3.060292
Intermediate Values	3.738295	0.026185	3.060292
Hot Spots	3.798074	0.024741	3.060292

Table 3.3. Summary of t-test results.

	t	*df*	*p-value*	Reject?
Cold Spots	2.062	142	0.041	**Reject**
Intermediate	-1.431	142	0.155	Fail to Reject
Hot Spots	2.089	142	0.038	**Reject**

After examining the scatterplots of the weekly and monthly average values (Figures 3.3 and 3.4) linear regression was used to examine the pattern of covariance between PMI and hot spots, cold spots, and intermediate elevation values. The general trend in the data suggests that the area of cold spots and hot spots decreases as PMI increases, and as a consequence the area of intermediate elevation increases as PMI

increases. Linear regression using all 144 fracture surfaces grouped by week results in almost no correlation (R^2) between PMI and cold spots ($R^2 = 0.08$), PMI and intermediate elevation ($R^2 = 0.07$), or PMI and hot spots ($R^2 = 0.07$). Linear regression using all 144 fracture surfaces grouped by month rather than week results in even lower correlations ($R^2 = 0.07, 0.06, 0.06$, respectively). These results clearly show that when all of the specimens are taken into account, there is almost no correlation between length of time and cold spots, intermediate elevation, or hot spots. Since the ANOVA test suggested that the monthly changes were not significant, these regression results are not unexpected.

Linear regression was also performed using average values for weeks and then again with averages for each month. When each week was averaged, the sample size dropped from 144 to 37. Plots illustrating the weekly average changes in cold spots, intermediate values, and hot spots with time with linear regression lines are shown in Figure 3.5. Using averages for each week slightly increased the correlation to 0.12 for cold spots, 0.09 for intermediate elevations, and 0.10 for hot spots. However, these correlations are still quite low, even after calculating averages to reduce the range of variance for each variable.

When the sample size was reduced to ten by averaging the values for each month (Figure 4), the correlation only increased to 0.54 for cold spots, 0.49 for intermediate values, and 0.46 for hot spots. Using averages to decrease the sample size from 144 to ten greatly reduces the amount of variability for the dependent variable and inevitably leads to an artificial increase in R^2 values. Yet even with this significant reduction in variation, only about half of the variation in the cold spots, intermediate values, and hot spots can

be explained by time. This suggests that while there appears to be a trend toward a flatter surface as the PMI increases, time is not explaining much of the variation.

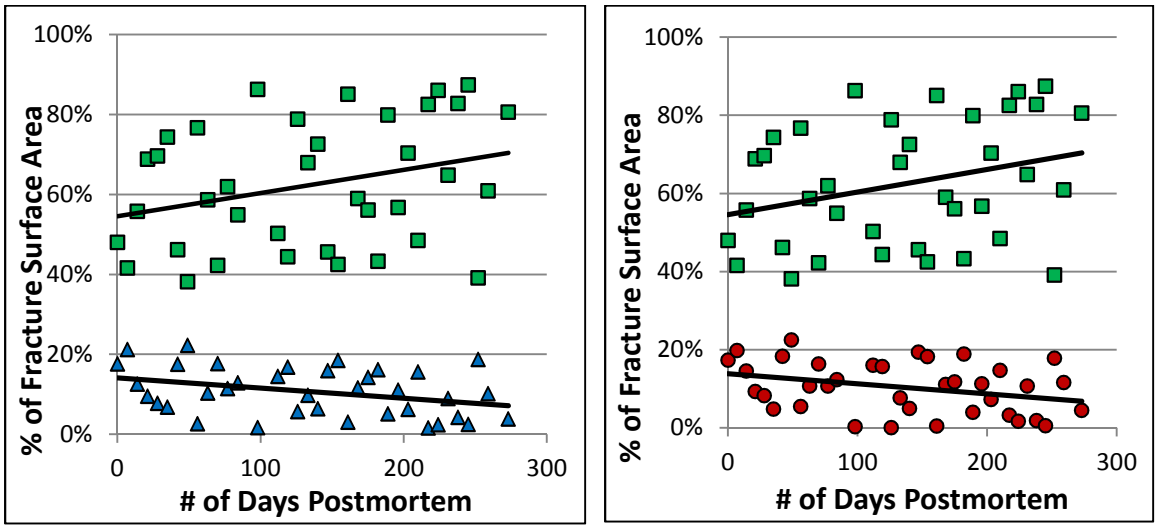

Figure 3.5. Scatterplots of weekly averaged values with linear regression lines. The plot on the left illustrates the cold spots (blue) and intermediate values (green), while the plot on the right illustrates the hot spots (red) and intermediate values (green).

CHAPTER IV

Discussion and Conclusion

With technology advancing every day, 3D surface scanners are becoming more ubiquitous as a part of the forensic anthropologist's toolbox. At the same time, in recent years there has also been an influx of the use of Geographic Information Systems (GIS) in anthropology. Geographic Information Systems software is designed to analyze spatial data associated with specific points on the surface of the Earth (Longley et al., 2005), yet anthropologists have discovered its applicability to address questions regarding functional morphology, histology, and scavenging activity (Ungar and Williamson, 2000; Rose et al., 2012; Spradley et al., 2012). The current study utilizes both of these technologies to address an age-old problem in forensic anthropology: the interpretation of the timing of skeletal trauma. Of particular importance to the forensic anthropologist is the ability to distinguish between perimortem and postmortem fractures, as perimortem fractures occur around the death event and may shed light on the circumstances surrounding an individual's death. Although certain gross characteristics can provide clues to differentiate between perimortem and postmortem fractures (e.g. fracture angle, fracture edge, fracture surface), these characteristics are non-quantifiable and often based on whether the bone was wet or dry at the time of fracturing. This study used a NextEngine© 3D scanner to scan the tension fracture surface of bones broken throughout the postmortem interval, and then GIS software was used to analyze, quantify, and track the changes to the fracture surface morphology across the postmortem interval.

Results of this study found that in general, the fracture surfaces had gradual decreases in hot and cold spots (hills and valleys) and gradual increases in intermediate elevation (flat land) over time. Put simply, bones broken earlier in the postmortem interval had rougher fracture surfaces with more areas of hills and valleys compared to bones broken later in the postmortem interval. As the postmortem interval increased, fracture surfaces generally had less hills and valleys and became smoother. This consistent patterning of hot and cold spots on the fracture surface suggests that osteonal pullouts are in fact being represented on the fracture surface.

Despite the overall trends in the data, analysis of variance found that the areas of hot spots, cold spots, and intermediate elevations were not significantly different when evaluated at monthly intervals. Nevertheless, when these features were compared across the early, middle, and late decomposition stages, they became statistically significant. These results imply that the changes to fracture surface morphology do not occur in discrete temporal intervals but rather they occur gradually, although not necessarily continuously. Indeed, previous research (e.g. Wheatley, 2008; Wieberg and Wescott, 2008; Shattuck, 2010) has shown that bones may remain green for an extended period of time, and that the drying process persists for several months after death. Consequently, the characteristics of the fracture (fracture angle, surface, and edge) change as the properties of the bone are slowly altered. Thus, the findings from this study support the notion that there is a continuous transition in fracture characteristics throughout the postmortem interval. In addition, these results suggest that it is nearly impossible to pigeonhole fracture characteristics into short temporal categories.

The linear regression analyses found no significant correlations between months in the postmortem interval and the areas of hot spots, cold spots, or intermediate elevations. However, even when the sample sizes were averaged and reduced to ten, there was still low correlation between time and the fracture surface features ($R^2 = 0.54$ for cold spots, 0.49 for intermediate values, and 0.46 for hot spots). Averaging the values for each month artificially increases the goodness of fit by reducing the variation in the samples, and yet after doing so the correlation between these features and time remained relatively low. This is interesting because the general trend in the data suggests that the area of cold spots and hot spots decreases as the postmortem interval increases, and that the area of intermediate elevation increases as the postmortem interval increases. So although there are visible trends in the data, time is not a major causal factor, although it may be a related factor. There could be multitudes of variables (e.g. bone moisture content, type of fracture) influencing the morphology of the fracture surface. In addition, the variation may also be attributed to the scale and resolution of the maps. It is possible that the resolution was too high to definitively answer the questions posed to the data. Future studies should look at scale and resolution and their effect on the outcome of an analysis such as this.

According to the results of the t-tests, intermediate elevation values were not significantly different between bones fractured during the first two months and those fractured after two months (Table 3.1). This is interesting because the results of the ANOVA found that the intermediate elevation was significantly different when broken up into months representing early, middle, and late decomposition. The t-test was not significant because combining months 3-10 created more variation within the group and

lessened the variation between the two groups. Although intermediate elevation values on either end of the postmortem interval were distinct, the values for the middle of the postmortem interval had considerable variation. This may be a reflection of the fracture surface features showing both perimortem and postmortem characteristics. In fact, the studies by Wieberg and Wescott (2008) and Shattuck (2010) found that bone fractures may present both perimortem and postmortem characteristics well into the postmortem interval. Wieberg and Wescott (2008) noted that even after five months no fractures presented exclusive postmortem characteristics. Therefore, it is possible that the t-test was not significant because the intermediate elevation was exhibiting a mixture of wet and dry characteristics.

It is also important to note that aside from time, there are many potential sources of variation in this study. One influencing factor could be that different types of fractures were used for this study rather than limiting the analysis to one type fracture. Another potential source of variation could be that the force fracturing the bones was not necessarily uniform. In addition, even though the same apparatus was used to break each specimen, the anatomical locations of the impact site varied. Finally, the side of the bone fractured may introduce variation because of differential drying. For instance, the side of the bone against the ground may have been wetter than the side exposed to the air and sun, and as a result the bone's response to fracturing was governed by whichever side (ground or air-exposed) was impacted. Therefore, the variation in this study could come from numerous uncontrolled sources.

The results of this analysis are interesting when put in context of previous research. Many authors have noted that fresh bone fractures have smooth fracture

surfaces and dry bone fractures have rough, jagged fracture surfaces (Johnson, 1985; Villa and Mahieu, 1991; Sauer, 1998; Wheatley, 2008; Wieberg and Wescott, 2008; Shattuck, 2010). Yet, the results of this analysis are in stark contrast to this traditional concept. The reason behind this contradiction may be due in large part to the fact that these morphological descriptions are macroscopic in nature. In fact, the results of this analysis are actually in agreement with the findings of Shipman (1981), who used scanning electron microscopy to examine perimortem and postmortem fracture surfaces. Shipman (1981) reports that microscopic perimortem fracture surfaces appear roughened with string-like structures because adjacent collagen bundles are pulled apart during the fracturing process. Similarly, the osteonal pull-out that Hiller and colleagues (2003) describe also likely contributes to the rough perimortem fracture surface. When placed under tension, osteons debond from the interstitial matrix to bridge the advancing crack until failure occurs and they are pulled out of the fracture surface in a telescoping fashion (Figure 1.3). Thus, it is possible that the perimortem fracture surface gets its roughened appearance from torn collagen bundles and osteonal pullout. As the bone dries and the collagen degrades, the bone is no longer able to fracture by pulling apart collagen fibers and instead the fracture occurs perpendicular to the collagen direction, which creates a more stepped appearance (Shipman, 1981). Similarly, as the osteons dry out they become less elastic and more brittle, so when the dry osteons are placed under tension they will not stretch. Therefore, it would be expected that bones fractured while the bone is green would have a relatively smooth fracture outline while having a rough fracture tension surface. Postmortem fractures, on the other hand, will have a jagged fracture outline but a relatively smooth fracture tension surface.

It is also important to note that this study only scanned the tension fracture surface, which restricted the analysis to a small portion of the total fracture surface. Previous studies comparing perimortem and postmortem fractures utilized the entire fracture surface to achieve an overall impression of rough or smooth. Because tensile forces pull the bone apart, it is possible that the tension fracture surface has a rougher microscopic appearance than the compression or shear sides. Therefore, it is possible that the area of the fracture surface under examination may influence the determination of perimortem or postmortem, and thus could also be a factor in these results opposing those of previous studies. This is something that should be investigated in future research.

There were three questions addressed by this research. The first asked if there is a quantifiable difference in the tension fracture surface of bones broken at the time of death (PMI=0 days) and those broken after death. The second question asked if there are any visible changes in tension fracture surface characteristics as bones progress through the postmortem interval. The final question considered if fracture timing could be recognized based on fracture surface characteristics.

The results of this study showed that using hotspot analysis in GIS successfully quantifies the tension fracture surface by assessing statistically significant spatial clusters of high and low elevation values (hills and valleys). Results found that in general, the fracture surfaces had gradual decreases in hot and cold spots and gradual increases in intermediate elevation values over time. While this experiment does show that there are significant trends in the data, the results indicate that there is no precise way to definitively assign a fracture to a discrete category based on tension fracture surface.

Considerations

It is important to remember that this study utilized a preexisting collection for analysis. As a result, some of the information for each specimen was unknown or unavailable for use. For instance, the bones had no writing or markings on them, so the area of impact was not clearly defined before or after fracturing. This meant that the impact site, and therefore the areas of tension and compression, needed to be determined for each specimen before they could be used in this analysis. While every effort was made to properly identify the tension fracture surface, it is possible that it was incorrectly identified in a few cases. In addition, the tension fracture surface was sometimes indeterminable, which inevitably resulted in the specimen being excluded for analysis. The inability to definitively locate the impact site, coupled with the comminuted nature of many of the specimens, inevitably led to a serious reduction in sample size. In fact, of the 99 comminuted specimens in the collection, 59 were excluded from analysis because the areas of tension and compression could not be pinpointed on the fracture surface. Future studies would benefit by conducting experiments where all the bones are broken with the same type (e.g., three-point bending) and amount of force, in the same anatomical location, and with documentation of the impact sight and tension surface.

One drawback of this study was the overwhelming amount of time spent post-processing the scans to ready them for analysis in GIS. This was the process of aligning, trimming, fusing, and orienting each scanned model. Trimming was perhaps the most critical step for this analysis because it was wholly reliant on the user, and consequently had the most potential for user error. If the scan was trimmed too little or too much, the results would become inaccurate and unsound. Therefore, most of the post-processing

was spent meticulously trimming each scan down to just the tension fracture surface. Each specimen took about an hour and a half to scan and ready for analysis, and because there were 144 scans, this amounted to over 200 hours of data collection. If this study is to be replicated or expanded on in the future, the researcher should be aware of the amount of processing time that goes into the analysis.

A frustrating limitation of this study is that fracture surfaces, especially small portions of fracture surfaces, do not contain landmark data. As a result, it is impossible to directly overlay multiple fracture surfaces in GIS to examine how they change over time. Instead, analysis is restricted to using spatial analyst tools on each individual fracture surface and then comparing the results from each analysis. This is frustrating because GIS has the capability of directly overlaying map layers to calculate the differences between them, as long as the data are georeferenced (that is, as long as the data is attached to specific points on the Earth's surface). If there was a way to identify or create landmarks with fracture surface data, it would improve and expand the types of analysis available with GIS.

Similarly, the tools for analysis in GIS were limited by the output of the NextEngine© scanner. While the NextEngine© boasts eight different output file formats, only one is compatible for import into ArcGIS, the GIS software used in this study. This file type (.xyz) consists of thousands, if not tens of thousands, of X, Y, Z coordinate points that make up the scanned fracture surface. Even though the points were sometimes separated by 1/100 of a millimeter, the data were still in the format of discrete, discontinuous points called vector data. Although vector data has its benefits, it was limiting for this study because many tools in GIS operate only with raster (pixel) data.

While it is possible to interpolate a raster from point data, the conversion inevitably generalizes the original data and information is lost. This also ties into the problem of scale and resolution. Scale and resolution may be factors affecting the outcome of the analysis, but without further studies testing them, there is no way to definitively tell if the resolution was too high or low for this analysis.

Suggestions for Future Research

Future research would benefit from validation studies testing the inter- and intra-observer errors of this method. It is important to assess the intra- and inter-observer errors because they show how reliable the methods and results are. Intra-observer error could be tested by completely rescanning specimens already used and comparing how they classify a second time around. Similarly, the inter-observer error could be tested if someone else scanned, prepared, and analyzed the same specimens used in this analysis, and then compared their results to the results of this study. Although it was beyond the scope of this study, future studies could focus on creating sectioning points from the hotspot analysis results that effectively classify fracture surfaces as either wet or dry. The validity of these classification criteria could then be tested in blind studies using specimens broken at known times throughout the postmortem interval.

As many authors have pointed out, the fracture characteristics used to distinguish perimortem from postmortem fractures are largely based on the qualities of the bone tissue rather than the timing of injury (Ubelaker and Adams, 1995; Galloway et al., 1999; Wieberg and Wescott, 2008; Shattuck, 2010). The current study supported this observation, as the regression analyses indicated that time does not explain the variation

in the hot spots, cold spots, and intermediate elevations on the fracture surface. Future research could expand on the current study by investigating the relationship between the features on the fracture surface and ash weight percentage. In fact, Wieberg and Wescott (2008) found a significant positive correlation between ash weight percentage and fracture surface appearance of bones broken throughout the postmortem interval. Therefore, future studies could combine the methods from this study with those of Wieberg and Wescott (2008) to examine the relationship between time, the condition of the bone, and the GIS analysis of the fracture surface features (the hot spots, cold spots, and intermediate elevations on the fracture surface).

Similarly, new studies focusing on perimortem and postmortem fracture characteristics could examine the relationship between time, the fracture angle, fracture edge, and the GIS analysis of the fracture surface. This introduces more variables that may help control for some of the variation introduced by other factors in this study. In addition, future studies could also test to see if the type of fracture (e.g. butterfly, transverse, oblique) affects the tension fracture surface. These fractures are created from different forces, and as a result the tension fracture surfaces may be differentially affected. Ultimately, this could reveal if GIS analysis of fracture surface morphology only works accurately on certain types of fractures.

Finally, future studies could explore different tools and settings for the analysis of tension fracture surfaces in GIS. There are many hotspot analysis tools available in GIS, but this study used just one of them. It is possible that other tools may yield different, or better, results. A sensitivity test using different tools and different parameters for those tools would also be beneficial because it would be a step toward standardizing the

methodology. Similarly, future research could use sensitivity tests to try and determine the appropriate resolution level for study.

Conclusion

While certain gross characteristics of fractures can provide clues to distinguish perimortem from postmortem blunt force trauma, anthropologists do not have a way to reliably measure or calibrate these fracture characteristics. This study sought to address this issue by analyzing the tension fracture surface morphology with the spatial statistics tools available in GIS software. The purpose of this study was to develop a novel method that could be used to help establish the timing of the fracturing incident. This is important for medicolegal death investigations because a perimortem fracture implies the injury is associated with the death event.

The results of this study indicate that fracture surface appearance gradually transitions from rough to smooth as the postmortem interval increases. The results also indicate that the manifestation of fracture surface characteristics is determined by how wet or dry the bone was at the time of fracturing rather than time. As osteons dry out they lose their elasticity, so when they are placed under tension they will not stretch. As a result, osteonal pullout will not occur in dry bone, and therefore, dry bone has a relatively smooth tension fracture surface compared to wet bone. The fact that the physical condition of the bone determines the fracture characteristics suggests that it is unreliable to assign a fracture to a discrete category because the transition from wet to dry is ambiguous.

REFERENCES CITED

Adams B, Crabtree P. 2012. Comparative osteology: a laboratory and field guide of common North American animals. Oxford: Academic Press.

Aufderheide AC, Rodriguez-Martin C. 1998. The Cambridge encyclopedia of human paleopathology. Cambridge: Cambridge University Press.

Behrensmeyer AK. 1978. Taphonomic and ecologic information from bone weathering. Paleobiology 4:150-162.

Bell LS, Skinner MF, Jones SJ. 1996. The speed of post mortem change to the human skeleton and its taphonomic significance. Forensic Science International 82(2):129-140.

Bonnichsen R, Will RT. 1980. Cultural modification of bone: the experimental approach in faunal analysis. In: Gilbert BM, ed. Mammalian osteology. Columbia, MO: Missouri Archaeol Soc. p. 7-30.

Currey JD. 1959. Differences in the tensile strength of bone of different histological types. J Anat 93:87-95.

Currey JD. 1970. The mechanical properties of bone. Clin Orthop Rel Res 73:210-231.

Daubert v. Merrell Dow Pharmaceuticals, Inc., 509 U.S. 579.

DeMers MN. 2009. Fundamentals of Geographic Information Systems. 4th ed. Hoboken, NJ: John Wiley and Sons, Inc.

Dirkmaat DC, Cabo LL, Ousley SD, Symes SA. 2008. New perspectives in forensic anthropology. Am J Phys Anthropol 137(S47):33-52.

Evans FG. 1957. Stress and strain in bones: their relation to fractures and osteogenesis. Springfield, IL: Charles C Thomas.

Evans FG. 1973. Mechanical properties of bone. Springfield IL: Charles C Thomas.

Friess M. 2012. Scratching the surface? The use of surface scanning in physical and paleoanthropology. Journal of Anthropological Sciences 90:1-25.

Galloway A. 1999. The biomechanics of fracture production. In: Galloway A, ed. Broken bones: anthropological analysis of blunt force trauma. Springfield, IL: Charles C. Thomas. p. 35-62.

Galloway A, Symes SA, Haglund WD, France DL. 1999. The role of the forensic anthropologist in trauma analysis. In: Galloway A, ed. Broken bones: anthropological analysis of blunt force trauma. Springfield, IL: Charles C. Thomas, 1999. p. 5-31.

Gonza ER. 1982. Biomechanics of long bone injury. In: Gonza ER, Harrington IJ, Evans DC, eds. Biomechanics of musculoskeletal injury. Baltimore: Williams and Wilkins. p. 1-24.

Guidi G, Remondino F, Morlando G, Del Mastio A, Ucceddu F, Pelagotti A. 2007. Performance evaluation of a low cost active sensor for cultural heritage documentation. In: Gruen A, Kahmen H, eds. VIII Conference on Optical 3D Measurement Techniques 2:59-69.

Hiller LP, Stover SM, Gibson VA, Gibeling JC, Prater CS, Hazelwood SJ, Yeh OC, Martin RB. 2003. Osteon pullout in the equine third metacarpal bone: effects of ex vivo fatigue. J Orthopaed Res 21:481-488.

Janjua MA, Rogers TL. 2008. Bone weathering patterns of metatarsal v. femur and the postmortem interval in Southern Ontario. Forensic Science International 178:16-23.

Johnson E. 1985. Current developments in bone technology. In: Schiffer MB, ed. Advances in archaeological method and theory, vol. 8. Orlando: Academic Press. p. 157-235.

Kroman AM, Symes SA. 2013. Investigation of Skeletal Trauma. In: DiGangi EA, Moore MK. eds. Research methods in human skeletal biology. Oxford: Elsevier. p. 219-240.

Levine N. 2010. Crimestat: A spatial statistics program for the analysis of crime incident locations (v3.3). Houston: Ned Levine and Associates, and Washington, DC: National Institute of Justice.

Longley PA, Goodchild MF, Maguire DJ, Rhind DW. 2005. Geographical information systems and science. 2nd ed. West Sussex, England: John Wiley & Sons Ltd.

Maples WR. 1986. Trauma analysis by the forensic anthropologist. In: Reichs KJ, ed. Forensic osteology: advances in the identification of human remains. Springfield, IL: Charles C Thomas. p. 218-228.

Moraitis K, Spiliopoulou C. 2006. Identification and differential diagnosis of perimortem blunt force trauma in tubular long bones. Forensic Sci. Med. Pathol 2(4):221-228.

NextEngine 3D Laser Scanner [Internet]. NextEngine, Inc. [cited 2011 November 14]. Available from: http://www.nextengine.com

Rose DC, Agnew AM, Gocha TP, Stout SD, Field JS. 2012. Technical note: the use of Geographic Information Systems software for the spatial analysis of bone microstructure. Am J Phys Anthropol 148:648-654.

Sauer NJ. 1998. The timing of injuries and manner of death: distinguishing among antemortem, perimortem and postmortem trauma. In: Reichs KJ, ed. Forensic osteology: advances in the identification of human remains. Springfield, Illinois: Charles C Thomas. p. 321-332.

Shattuck RE. 2010. Perimortem fracture patterns in south-central Texas: a preliminary investigation into the perimortem interval. MA thesis, Texas State University, Department of Anthropology.

Shipman P. 1981. Applications of scanning electron microscopy to taphonomic problems. Annals of the New York Academy of Sciences 376:357-386.

Slizewski A, Friess M, Semal P. Surface scanning of anthropological specimens: nominal-actual comparison with low cost laser scanner and high end fringe light projection surface scanning systems. Quartär 57:179-187.

Smith OC, Pope EJ, Symes SA. 2003. Look until you see: identification of trauma in skeletal material. In: Steadman DW, ed. Hard evidence: case studies in forensic anthropology. Upper Saddle River, NJ: Prentice Hall. p. 138-154.

Spradley MK, Hamilton MD, Giordano A. 2012. Spatial patterning of vulture scavenged human remains. Forensic Science International 219:57-63.

Tucker BK, Hutchinson DL, Gilliland MF, Charles TM, Daniel HJ, and Wolfe LD. 2001. Macroscopic characteristics of hacking trauma. J Forensic Sci 46:234-240.

Ubelaker DH, Adams BJ. 1995. Differentiation of perimortem and postmortem trauma using taphonomic indicators. J Forensic Sci 40(3):509-512.

Ungar P, Williamson M. 2000. Exploring the effects of toothwear on functional morphology: a preliminary study using dental topographic analysis. Palaeontologia Electronica 3:1-18.

Villa P, Mahieu E. 1991. Breakage patterns of human long bones. J Human Evol 21:27-48.

Wheatley BP. 2008. Perimortem or postmortem bone fractures? An experimental study of fracture patterns in deer femora. J Forensic Sci 53(1):69-72.

White TD, Black MT, Folkens PA. 2012. Human osteology. 3rd ed. Burlington, Massachusetts: Elsevier Academic Press.

Wieberg DA, Wescott DJ. 2008. Estimating the timing of long bone fractures: correlation between the postmortem interval, bone moisture content, and blunt force trauma fracture characteristics. J Forensic Sci 53(5):1028-1034.